CURRENT ONCOLOGY
A Canadian Cancer Research Journal

Digital gene expression analysis might aid in the diagnosis of thyroid cancer

H. Armanious MD PhD,*† B. Adam MD,*† D. Meunier MD,*† K. Formenti BSc,† and I. Izevbaye MBBS PhD*†

ABSTRACT

Background Thyroid cancer represents approximately 90% of endocrine cancers. Difficulties in diagnosis and low inter-observer agreement are sometimes encountered, especially in the distinction between the follicular variant of papillary thyroid carcinoma (FvPTC) and other follicular-patterned lesions, and can present significant challenges. In the present proof-of-concept study, we report a gene-expression assay using NanoString nCounter technology (NanoString Technologies, Seattle, WA, U.S.A.) that might aid in the differential diagnosis of thyroid neoplasms based on gene-expression signatures.

Methods Our cohort included 29 patients with classical papillary thyroid carcinoma (PTC), 13 patients with FvPTC, 14 patients with follicular thyroid carcinoma (FTC), 14 patients with follicular adenoma (FA), and 14 patients without any abnormality. We developed a 3-step classifier that shows good correlation with the pathologic diagnosis of various thyroid neoplasms. Step 1 differentiates normal from abnormal thyroid tissue; step 2 differentiates benign from malignant lesions; and step 3 differentiates the common malignant entities PTC, FTC, and FvPTC.

Results Using our 3-step classifier approach based on selected genes, we developed an algorithm that attempts to differentiate thyroid lesions with varying levels of sensitivity and specificity. Three genes—namely *SDC4, PLCD3*, and *NECTIN4/PVRL4*—were the most informative in distinguishing normal from abnormal tissue with a sensitivity and a specificity of 100%. One gene, *SDC4*, was important for differentiating benign from malignant lesions with a sensitivity of 89% and a specificity of 92%. Various combinations of genes were required to classify specific thyroid neoplasms.

Conclusions This preliminary proof-of-concept study suggests a role for nCounter technology, a digital gene expression analysis technique, as an adjunct assay for the molecular diagnosis of thyroid neoplasms.

Key Words Thyroid neoplasms, papillary thyroid carcinoma, follicular neoplasms, gene expression profiling, NanoString

Curr Oncol. 2020 April:27(2)e93–e99   www.current-oncology.com

INTRODUCTION

Thyroid cancer represents approximately 90% of endocrine cancers[1]. Thyroid cancers are classified into distinct types, including papillary thyroid carcinoma (PTC), follicular variant of papillary thyroid carcinoma (FvPTC), follicular adenoma (FA), and follicular thyroid carcinoma (FTC). The most common of these lesions is PTC. Surgical pathology diagnosis of PTC, largely dependent on nuclear features, is usually straightforward; nevertheless, those cytologic criteria are subjective, with no uniform minimum diagnostic criteria[2,3].

Diagnostic dilemmas are sometimes encountered in which the distinction between FvPTC and other follicular-patterned lesions presents challenges[4]. Occasionally, nuclear features are not sufficiently developed for an unequivocal diagnosis of PTC[5]. Difficulties also attend the differentiation of subtypes of follicular lesions, including separating reactive lesions such as adenomatous goiter and Hashimoto thyroiditis from neoplastic conditions such as FA. Given the differences in prognosis and management for those entities, accurate diagnosis is imperative.

The diagnostic challenges encountered in the assessment of thyroid lesions are demonstrated by significant

inter-observer variability, with observer agreement being as low as 58% in some studies[6–9]. Factors implicated by such studies include the interpretive significance of microfollicles and capillaries within tumour capsules, variations in the assessment of nuclear features such as nuclear clearing for PTC, and lack of strict criteria for distinguishing adenomatous goiter and FA.

Various attempts to address these common diagnostic challenges have been made. Past approaches have largely been confined to the use of various immunohistochemical stains, singly and in combination. Numerous antibodies have been explored—including those against HBME-1, CK19, galectin-3, galectin-1, CITED-1, CD44, Trop-2, CD56, and TPO—with varying degrees of success[4,10–19]. Previous investigators have also assessed the utility of immuno-histochemistry for confirming malignancy, identifying vascular invasion in follicular lesions, and differentiating FvPTC from FA[20–23]. However, immunohistochemistry is also confounded with issues of inter-observer sensitivity and specificity and inter-laboratory variation in application.

A genomics study from The Cancer Genome Atlas (TCGA) has proposed the classification of thyroid cancers based on molecular subtypes that better reflect the biologic pathways involved with each cancer subtype[24]. Using gene-expression profiling (GEP), that project was able to identify unique gene signatures for PTC. Molecular methods using next-generation sequencing (ThyroSeq: UPMC, Pittsburgh, PA, U.S.A.) and GEP (Affirma: Thermo Electron Scientific Instruments, Madison, WI, U.S.A) are established adjunct methods in indeterminate thyroid cytology. Those genomics technologies have thus far been limited to thyroid cytology. Their implementation in routine surgical pathology has been hampered because of prohibitive operational and infrastructural costs. Some investigators have also used gene-expression techniques such as DNA microarrays to identify biomarkers of PTC, FTC, and FA. However, those studies have been largely investigational and have not as yet been translated into a clinical assay for routine use in surgical pathology[25,26].

In the present proof-of-concept study, we used a rapid, cost-effective digital counting technology, nCounter (NanoString Technologies, Seattle, WA, U.S.A.) for gene-expression analysis. We identified diagnostic biomarkers and developed a preliminary diagnostic algorithm that might aid in resolving diagnostically challenging cases in the surgical pathology assessment of thyroid neoplasms.

METHODS

Thyroid Samples
This study was approved by the Health Research Ethics Board of Universities of Alberta and Calgary.

The laboratory information system at the University of Alberta and Royal Alexandra hospitals in Edmonton, Alberta, were searched for all patients with a diagnosis of thyroid neoplasm between January 2010 and December 2016. That search identified 81 patients with thyroid neoplasms and 14 patients with normal results. Predetermined sample inclusion criteria were a tumour area of 5 mm or more[2], tumour cellularity of 80% or more, RNA quantity 100 ng or more, and satisfactory intrinsic quality control metrics in

the nSolver analysis software (NanoString Technologies) for gene expression.

The 70 samples that met the inclusion criteria (86%) included 42 of PTC (including 29 classical PTC and 13 FvPTC), 14 of FTC, and 14 of FA. The PTC cases were separated into classical PTC and FvPTC because previous publications have shown differences in the biologic behavior of those two groups[27,28]. The PTC group included only the classical type; other variants of PTC were excluded because too few cases were identified for statistical analysis. The FvPTC cases included encapsulated minimally or widely invasive; the diagnosis of noninvasive follicular thyroid neoplasm with papillary-like nuclear features could not be made in any of the encapsulated cases because the entire capsule was not assessed during initial tissue processing. The normal-results group included multinodular hyperplastic thyroid tissue. Other reactive lesions such as Hashimoto thyroiditis were excluded. Archival formalin-fixed paraffin-embedded tissue (FFPE) blocks were retrieved for all study samples. One hematoxylin and eosin–stained section and five 10-μm unstained slides of diagnostic tissue were prepared. The stained tissue sections were reviewed by a pathologist (HA), and an area of high tumour cellularity (>80%) was identified and circled. Corresponding tissue was then macrodissected from unstained slides for RNA extraction.

RNA Isolation
The RNeasy FFPE kit (Qiagen, Hilden, Germany) was used to isolate RNA from five 10-μm sections from each sample. The RNA concentration and purity were measured using a NanoDrop 2000 spectrophotometer (Thermo Fisher Scientific, Waltham, MA, U.S.A.).

Code Set Design
A literature search was performed to identify genes involved in thyroid cancer biology, and TCGA was also reviewed[24]. Key words for our literature search included "thyroid carcinoma," "gene expression," "FTC," "gene profiling," "PTC," "follicular neoplasms (FN)," "FvPTC," and "FA," singly and in combination. The 83 genes selected as a result included 5 housekeeping genes: *ACAT2, ACTB, ATF4, RPL27,* and *RPS13.* The gene set included all 71 genes in the thyroid differentiation signature identified by TCGA. Custom nCounter probes for the gene set were designed by NanoString Technologies and manufactured by Integrated DNA Technologies [Coralville, IA, U.S.A. (supplemental Table 1)].

Expression Quantification
Details of the nCounter technology have been reported previously[29]. Briefly, a custom nCounter code set consisting of multiplexed probes targeting the 83-gene set, were used for gene-expression analysis. Each code set includes selected housekeeping genes to control for variations in RNA input and quality.

Probe pairs with sequences specific to a 100-base region of each target messenger RNA were designed using a 3′ biotinylated capture probe and a 5′ reporter probe tagged with a specific fluorescent barcode, thus creating 2 sequence-specific probes for each target transcript. Probes were hybridized with RNA at 65°C, and then applied to the nCounter Preparation Station for automated removal

of excess probe and immobilization of probe-transcript complexes on a streptavidin-coated cartridge. Data were collected using the nCounter Digital Analyzer by counting the individual barcodes. Raw gene expression counts were quality-controlled and normalized using the nSolver Analysis Software (version 2.0: NanoString Technologies) and manufacturer-included positive and negative controls. Quality control (QC) parameters include imaging QC, binding density QC, overall assay efficiency, assay linearity, and limit of detection (supplemental text: QC parameters). Data were normalized to the 5 housekeeping genes to correct for variation in RNA input quantity.

Statistical Analysis

Post-normalization statistical analysis and visualization were performed with the R software application (version 3.3.2: R Foundation for Statistical Computing, Vienna, Austria). Normalized transcript counts were used for individual gene analysis (supplemental Table 2). Geometric means of normalized transcript counts were used for aggregate gene-set analysis. Exploratory analysis was performed using heat maps with unsupervised hierarchical clustering by Euclidean distance (heatmap.2 function in g plots package for R) and unsupervised principal component analysis (prcomp function in stats package for R). Receiver operating characteristic (ROC) curve analysis (roc function in pROC package for R) was used to assess individual gene and gene-set performance in each of the diagnostic scenarios. Individual genes were first ranked by area under the curve values and then compiled into respective upregulated and downregulated gene sets. That is, 1-gene set is the top gene; 2-gene set is the geometric mean of the top 2 genes; 3-gene set is the geometric mean of the top 3 genes; and so on. The ROC curve analysis was then repeated for each gene set and the one with the highest area under the curve was identified for each diagnostic scenario (in the event of a tie, the one with the most transcripts was selected). Benjamini–Hochberg (false discovery rate) correction for multiple comparisons was used for all differential expression analyses. Only genes with corrected *p* values or false discovery rates less than 0.05 were included in the gene sets. The Youden *J*-statistic (point on the ROC curve furthest from the diagonal index line) defined the diagnostic thresholds. Leave-one-out cross-validation analysis (train function in caret package for R) was used to validate individual gene and gene-set ROC results. Mann–Whitney *U*-tests (wilcox.test function in stats package for R) were used for diagnostic class comparisons. A *p* value less than 0.05 was considered statistically significant.

RESULTS

RNA and Quality Control

The mean RNA yield obtained from five 10 μm sections per FFPE block was 7480.6 ng (range: 161.4 ng–31204.4 ng) with a mean concentration of 374.03 ng/μL (8.07 ng/μL–1560.22 ng/μL) and a mean A260/A280 RNA purity ratio of 1.93.

Analytic Cohort of 84 Thyroid Cases

Of 95 identified samples with available paraffin-embedded material, 11 were excluded from downstream analysis because of quality control (*n* = 5) or normalization (*n* = 6)

flags encountered during nSolver processing. Gene expression data were adequate for 84 of 95 samples (88%) using FFPE material, and those samples constituted the analytic cohort for the study.

Gene Expression Cluster Analysis Shows Clustering of PTC Compared with Other Lesions Using 78-Gene Set

Using all 78 genes and all 84 samples, hierarchical clustering identified molecular signatures for 3 diagnostic groups: PTC, follicular neoplasms, and normal thyroid tissue. Papillary thyroid cancer appears to be molecularly distinct and clustered with 100% specificity within the PTC signature, which contained both classical PTC and some FvPTC samples. The follicular neoplasms cluster included FvPTC, FTC, and FA [Figure 1(A)]. Normal thyroid tissue samples were predominantly clustered together with some overlap with PTC, FA, and FTC. Using all 78 genes and all 84 samples, principal component analysis demonstrated findings similar to those for the heat-map analysis—that is, the genes mainly separated PTC from "not PTC" with FvPTC cases scattered between both groups [Figure 1(B)].

A 3-Step Gene Expression Algorithm Classifies Thyroid Lesions

We developed a 3-step algorithm for diagnostic classification: Step 1 distinguishes normal thyroid samples (*n* = 14) from abnormal (*n* = 70), including benign FA and malignant lesions (PTC, FTC). Step 2 differentiates benign tissue from malignant, and step 3 subclassifies malignant lesions.

Step 1 Analysis

We divided the cohort of 84 patients into 2 groups: normal (*n* = 14) and abnormal (*n* = 70). The 78-gene panel was then used to evaluate gene expression. The ROC analysis of the results identified 3 genes—*SDC4*, *PLCD3*, and *PVRL4*—to be the combination of genes with the best discriminatory value between those diagnostic groups, with test performance sensitivity, specificity, and area under the curve being 100% (Figure 2).

Step 2 Analysis

The cohort of 84 patients was stratified into 2 groups: benign, including normal tissue (*n* = 14) and FA (*n* = 14), and malignancy (PTC, FTC; *n* = 56). The 78-gene panel was then used to evaluate gene expression. The ROC analysis identified the gene *SDC4* (alone and not in combination with any other gene) to be the most discriminatory between the cohorts, with test performance sensitivity of 89%, specificity of 92%, and positive predictive value of 98% (Figure 3).

Step 3 Analysis

Finally, the 56 malignant thyroid lesion samples were separated into 3 groups: classic PTC (*n* = 29), FTC (*n* = 14) and FvPTC (*n* = 13). The 78-gene panel was then used to evaluate gene expression. The ROC analysis identified 3 gene sets that were differentially expressed in the groups (supplemental Table 3). A 13-gene set *(SPOCK2, KCNN4, AHR, RUNX1, FN1, CTSC, ITGB8, PTPRE, ANXA2P2, PDLIM4, SLC34A2, CFH, STK17B)* was most discriminatory between classical PTC compared with FTC and FvPTC. A 3-gene set *(CA12, CYB561,*
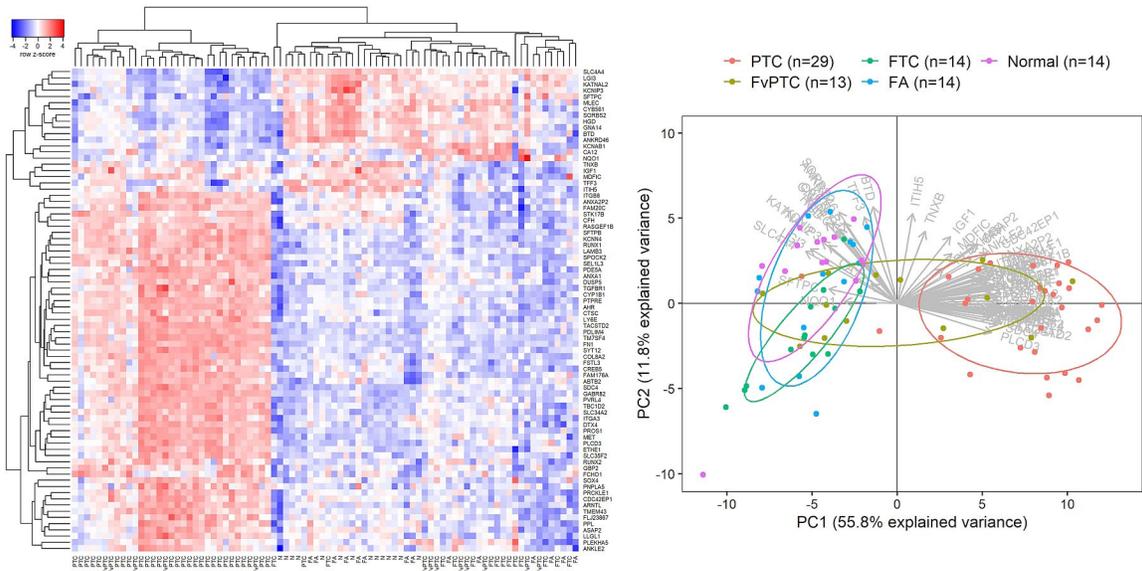
FIGURE 1 (A) With inclusion of the entire 83-gene panel, heat-map analysis demonstrates unsupervised hierarchical clustering of papillary thyroid carcinoma (PTC), follicular thyroid carcinoma (FTC), normal thyroid, follicular variant of papillary thyroid carcinoma (FvPTC), and follicular adenoma (FA) samples. Columns show genes; rows show patient samples. Blue shows downregulation of gene expression; red shows upregulation of gene expression. (B) Principal component (PC) analysis including all 78 genes and all 84 samples. No significant separation between FTC, FA, and normal is observed, with PTC appearing molecularly distinct from those three categories, and FvPTC overlapping PTC and "not PTC."
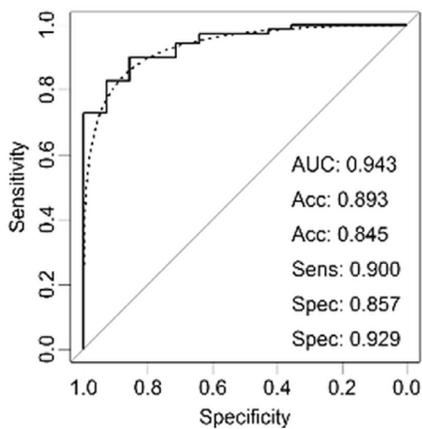

FIGURE 2 Three genes differentiate "normal" from "not normal." For each diagnostic group comparison, a receiver operating characteristic analysis was performed for each individual gene. The top upregulated gene set [highest area under the curve (AUC)] is shown. Acc = accuracy; Sens = sensitivity; Spec = specificity.
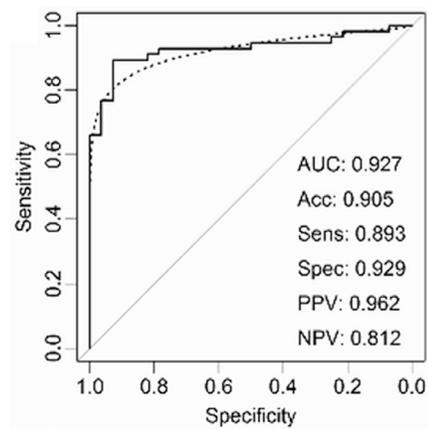

FIGURE 3 *SDC4* differentiates benign from malignant lesions. The top upregulated single-gene set is shown. AUC = area under the curve; Acc = accuracy; Sens = sensitivity; Spec = specificity; PPV = positive predictive value; NPV = negative predictive value.

KCNAB1) was most discriminatory between classical FvPTC compared with PTC and FTC. A single gene, *SLC4A4*, was most discriminatory between classical FTC compared with FvPTC and PTC (Figure 4).

The gene sets that are most discriminatory between each of the malignant groups (Figure 5) are a 2-gene set differentiating PTC and FvPTC *(SPOCK2, FN1)*, a 7-gene set differentiating PTC and FTC *(SPOCK2, KCNN4, ITGB8, LY6E, PTPRE, CFH, PDE5A)*, and a 9-gene set differentiating FTC and FvPTC *(KCNN4, PDE5A, SDC4, ANXA1, SEL1L3, GABR82, TBC1D2, DUSP5, CREB5)*.

DISCUSSION

In the present study, we report a proof-of-principle gene expression approach using NanoString nCounter technology as an adjuvant test for classifying thyroid neoplasms. The genes included in the study were selected from publicly available gene expression data sources, including TCGA, and a literature review of PubMed. Unsupervised hierarchical clustering of our gene expression results delineated 3 molecular signatures, 1 highly specific for PTC, as previously demonstrated by TCGA, and 2 relatively less-specific signatures for follicular lesions and normal tissue.
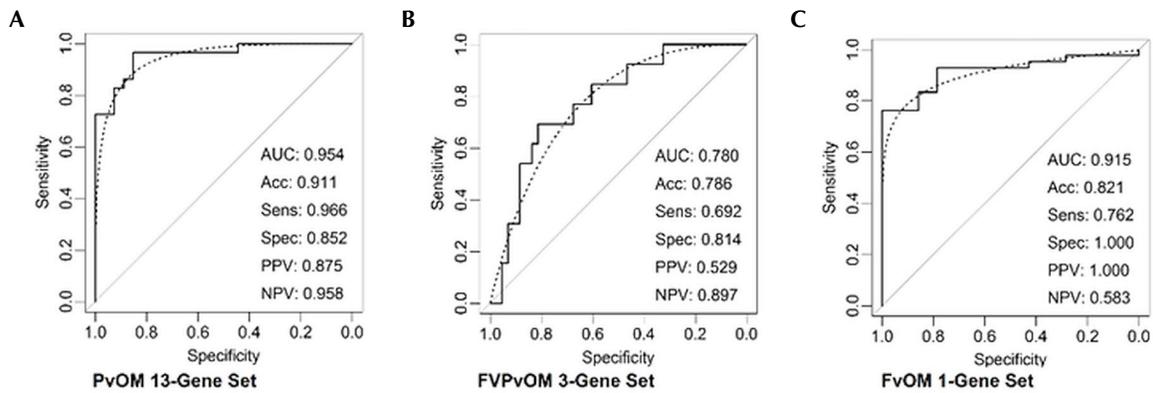
FIGURE 4 Top upregulated gene sets differentiate specific thyroid neoplasms from others: (A) 13 genes differentiate papillary (P) thyroid carcinoma from other malignancies (OM); (B) 3 genes differentiate the follicular variant of papillary (FVP) thyroid carcinoma from other malignancies (OM); and (C) 1 gene differentiates follicular (F) thyroid carcinoma from other malignancies (OM). AUC = area under the curve; Acc = accuracy; Sens = sensitivity; Spec = specificity; PPV = positive predictive value; NPV = negative predictive value.

FIGURE 5 Top upregulated gene sets differentiate specific thyroid neoplasms from others: (A) 7 genes differentiate papillary (P) from follicular (F) thyroid carcinoma; (B) 2 genes differentiate classical papillary (P) thyroid carcinoma from the follicular variant of papillary (FVP) thyroid carcinoma; (C) 9 genes differentiate the follicular variant of papillary (FVP) thyroid carcinoma from classical follicular (F) thyroid carcinoma. AUC = area under the curve; Acc = accuracy; Sens = sensitivity; Spec = specificity; PPV = positive predictive value; NPV = negative predictive value.
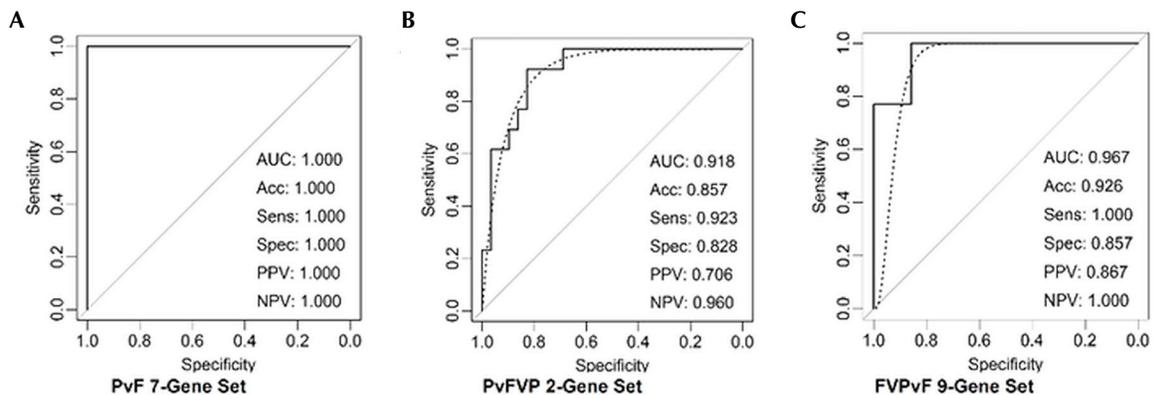
A 3-step classifier was able to improve the diagnosis of the other classes of thyroid neoplasms. Using the 3-step classifier approach based on selected genes, we were able to differentiate various tissue categories, including normal compared with abnormal; benign compared with malignant; and distinct malignant entities, including PTC, FvPTC, and FTC. Three genes, *SDC4, PLCD3,* and *PVRL4,* were most informative in distinguishing normal from abnormal tissue with a sensitivity and specificity of 100%; *SDC4* was most important for differentiating benign from malignant, with a sensitivity of 89% and a specificity of 92%. Various combinations of genes were required to classify specific thyroid neoplasms.

Many of the genes that we identified as being most discriminatory in our study have previously been shown by other authors to be of significance in this context. *SDC4* has been shown in various studies to be highly expressed in thyroid carcinoma compared with normal samples[30–32]. *SLC4A4,* which in our study showed significant differential expression between FTC and other types of cancers, has been used in a 15-gene set for differentiating benign from malignant samples in indeterminate cytology specimens[33].

That result is especially promising in the otherwise challenging histologic distinction between cases of FTC and FvPTC. *SLC4A4* could potentially serve as a distinguishing biomarker if validated as an immunohistochemical stain.

Our study demonstrates the potential utility of nCounter technology as an adjunct assay for clinical molecular diagnosis of thyroid neoplasms. NanoString is an innovative technique for the rapid digital assessment of gene expression that is amenable to in-house clinical implementation because of simplicity of use, efficient workflow, cost effectiveness, and user-friendly bioinformatics analysis. The successful analysis of 84 from among 95 of our archival FFPE samples (88%) demonstrates the robustness and efficacy of the technique for surgical pathology specimens. To date, the complexity of other methods for GEP, such as DNA microarrays and RNA sequencing, present significant challenges for the widespread clinical laboratory adoption of such techniques as an ancillary in-house assay. Gene-expression profiling using NanoString is amenable to in-house implementation by smaller laboratories with limited resources. In a number of disease entities, GEP has been adopted clinically for diagnostic, predictive,

and prognostic indications, including determining the cell of origin in diffuse large B-cell lymphoma and identifying the primary site of tumours of unknown origin[34,35]. And GEP has also been demonstrated to be a useful prognostic and predictive tool in breast carcinoma[36,37], brain[38] and gastric cancers[39], and melanomas[40].

NanoString is particularly suitable for the highly degraded nucleic acid material derived from FFPE samples, which is the standard processing method used in the surgical pathology assessment of thyroid neoplasms. Our results demonstrate good sensitivity and specificity in thyroid diagnosis, but limitations of this preliminary study include the use of only a limited training-sample cohort. Thus, the performance characteristics of sensitivity and specificity have not been definitively established. More extensive validation in an independent validation cohort is required to establish the performance characteristics (including positive and negative predictive value) and to investigate use of the technique as both a "rule in" and a "rule out" test. To assess the clinical utility of our classifier assay in diagnostic pathology, the validation cohort should include diagnostically challenging cases and other reactive thyroid lesions such as Hashimoto thyroiditis.

CONCLUSIONS

Using the NanoString nCounter platform, we developed a 3-step gene-expression classifier assay for the diagnosis of thyroid neoplasms. This classifier has potential utility in diagnostically challenging cases of thyroid lesions.

CONFLICT OF INTEREST DISCLOSURES
We have read and understood *Current Oncology*'s policy on disclosing conflicts of interest, and we declare the following interests: II has received honoraria for serving on advisory boards for AstraZeneca, Pfizer, Bayer, Novartis, and PrecisionRx-Dx. All other authors have no conflicts to disclose.

AUTHOR AFFILIATIONS
*Department of Laboratory Medicine and Pathology, University of Alberta, and †Alberta Public Laboratories, University of Alberta, Edmonton, AB.

REFERENCES
1. Pellegriti G, Frasca F, Regalbuto C, Squatrito S, Vigneri R. Worldwide increasing incidence of thyroid cancer: update on epidemiology and risk factors. *J Cancer Epidemiol* 2013;2013:965212.
2. Chan J. Strict criteria should be applied in the diagnosis of encapsulated follicular variant of papillary thyroid carcinoma. *Am J Clin Pathol* 2002;117:16–18.
3. Renshaw AA, Gould EW. Why there is the tendency to "overdiagnose" the follicular variant of papillary thyroid carcinoma. *Am J Clin Pathol* 2002;117:19–21.
4. Vasko VV, Gaudart J, Allasia C, *et al.* Thyroid follicular adenomas may display features of follicular carcinoma and follicular variant of papillary carcinoma. *Eur J Endocrinol* 2004;151:779–86.
5. Williams ED. Guest editorial: two proposals regarding the terminology of thyroid tumors. *Int J Surg Pathol* 2000;8:181–3.
6. Franc B. Observer variation of lesions of the thyroid. *Am J Surg Pathol* 2003;27:1177–9.
7. Franc B, de la Salmoniere P, Lange F, *et al.* Interobserver and intraobserver reproducibility in the histopathology of follicular thyroid carcinoma. *Hum Pathol* 2003;34:1092–100.
8. Hirokawa M, Carney JA, Goellner JR, *et al.* Observer variation of encapsulated follicular lesions of the thyroid gland. *Am J Surg Pathol* 2002;26:1508–14.
9. Lloyd RV, Erickson LA, Casey MB, *et al.* Observer variation in the diagnosis of follicular variant of papillary thyroid carcinoma. *Am J Surg Pathol* 2004;28:1336–40.
10. Papotti M, Rodriguez J, De Pompa R, Bartolazzi A, Rosai J. Galectin-3 and HBME-1 expression in well-differentiated thyroid tumors with follicular architecture of uncertain malignant potential. *Mod Pathol* 2005;18:541–6.
11. Dunderovic D, Lipkovski JM, Boricic I, *et al.* Defining the value of CD56, CK19, galectin 3 and HBME-1 in diagnosis of follicular cell derived lesions of thyroid with systematic review of literature. *Diagn Pathol* 2015;10:196.
12. Erdogan-Durmus S, Ozcan D, Yarikkaya E, Kurt A, Arslan A. CD56, HBME-1 and cytokeratin 19 expressions in papillary thyroid carcinoma and nodular thyroid lesions. *J Res Med Sci* 2016;21:49.
13. Murtezaoglu AR, Gucer H. Diagnostic value of Trop-2 expression in papillary thyroid carcinoma and comparison with HBME-1, galectin-3 and cytokeratin 19. *Pol J Pathol* 2017;68:1–10.
14. Prasad ML, Pellegata NS, Huang Y, Nagaraja HN, de la Chapelle A, Kloos RT. Galectin-3, fibronectin-1, CITED-1, HBME1 and cytokeratin-19 immunohistochemistry is useful for the differential diagnosis of thyroid tumors. *Mod Pathol* 2005;18:48–57.
15. Scognamiglio T, Hyjek E, Kao J, Chen YT. Diagnostic usefulness of HBME1, galectin-3, CK19, and CITED1 and evaluation of their expression in encapsulated lesions with questionable features of papillary thyroid carcinoma. *Am J Clin Pathol* 2006;126:700–8.
16. Abdou AG, Shabaan M, Abdallha R, Nabil N. Diagnostic value of Trop-2 and CK19 expression in papillary thyroid carcinoma in both surgical and cytological specimens. *Clin Pathol* 2019;12:2632010X19863047.
17. Dong S, Xie XJ, Xia Q, Wu YJ. Indicators of multifocality in papillary thyroid carcinoma concurrent with Hashimoto's thyroiditis. *Am J Cancer Res* 2019;9:1786–95.
18. Zargari N, Mokhtari M. Evaluation of diagnostic utility of immunohistochemistry markers of Trop-2 and HBME-1 in the diagnosis of thyroid carcinoma. *Eur Thyroid J* 2019;8:1–6.
19. Cho H, Kim JY, Oh YL. Diagnostic value of HBME-1, CK19, galectin 3, and CD56 in the subtypes of follicular variant of papillary thyroid carcinoma. *Pathol Int* 2018;68:605–13.
20. Sadullahoglu C, Sayiner A, Suren D, *et al.* The diagnostic significance of trophoblast cell-surface antigen-2 expression in benign and malignant thyroid lesions. *Indian J Pathol Microbiol* 2019;62:206–10.
21. Mohamed DA, Shamlola MM. Immunohistochemical and morphometrical evaluation of well-differentiated thyroid tumor of uncertain malignant potential. *Indian J Pathol Microbiol* 2019;62:17–23.
22. Cracolici V, Parilla M, Henriksen KJ, Cipriani NA. An evaluation of CD61 immunohistochemistry in identification of vascular invasion in follicular thyroid neoplasms. *Head Neck Pathol* 2019;:[Epub ahead of print].
23. Pyo JS, Kim DH, Yang J. Diagnostic value of CD56 immunohistochemistry in thyroid lesions. *Int J Biol Markers* 2018;33:161–7.
24. Cancer Genome Atlas Research Network. Integrated genomic characterization of papillary thyroid carcinoma. *Cell* 2014;159:676–90.
25. Reyes I, Reyes N, Suriano R, *et al.* Gene expression profiling identifies potential molecular markers of papillary thyroid carcinoma. *Cancer Biomark* 2019;24:71–83.
26. Wang Q, Shen Y, Ye B, *et al.* Gene expression differences between thyroid carcinoma, thyroid adenoma and normal thyroid tissue. *Oncol Rep* 2018;40:3359–69.

27. Lee SR, Jung CK, Kim TE, *et al.* Molecular genotyping of follicular variant of papillary thyroid carcinoma correlates with diagnostic category of fine-needle aspiration cytology: values of *RAS* mutation testing. *Thyroid* 2013;23:1416–22.

28. Rivera M, Ricarte-Filho J, Knauf J, *et al.* Molecular genotyping of papillary thyroid carcinoma follicular variant according to its histological subtypes (encapsulated vs infiltrative) reveals distinct *BRAF* and *RAS* mutation patterns. *Mod Pathol* 2010;23:1191–200.

29. Veldman-Jones MH, Brant R, Rooney C, *et al.* Evaluating robustness and sensitivity of the NanoString Technologies nCounter platform to enable multiplexed gene expression analysis of clinical samples. *Cancer Res* 2015;75:2587–93.

30. Chen LL, Gao GX, Shen FX, Chen X, Gong XH, Wu WJ. *SDC4* gene silencing favors human papillary thyroid carcinoma cell apoptosis and inhibits epithelial mesenchymal transition via Wnt/beta-catenin pathway. *Mol Cells* 2018;41:853–67.

31. Chung KW, Kim SW, Kim SW. Gene expression profiling of papillary thyroid carcinomas in Korean patients by oligonucleotide microarrays. *J Korean Surg Soc* 2012;82:271–80.

32. Griffith OL, Melck A, Jones SJ, Wiseman SM. Meta-analysis and meta-review of thyroid cancer gene expression profiling studies identifies important diagnostic biomarkers. *J Clin Oncol* 2006;24:5043–51.

33. Gomez-Rueda H, Palacios-Corona R, Gutierrez-Hermosillo H, Trevino V. A robust biomarker of differential correlations improves the diagnosis of cytologically indeterminate thyroid cancers. *Int J Mol Med* 2016;37:1355–62.

34. Scott DW, Wright GW, Williams PM, *et al.* Determining cell-of-origin subtypes of diffuse large B-cell lymphoma using gene expression in formalin-fixed paraffin-embedded tissue. *Blood* 2014;123:1214–17.

35. Yoon N, Ahn S, Yong Yoo H, Jin Kim S, Seog Kim W, Hyeh Ko Y. Cell-of-origin of diffuse large B-cell lymphomas determined by the Lymph2Cx assay: better prognostic indicator than Hans algorithm. *Oncotarget* 2017;8:22014–22.

36. Gnant M, Filipits M, Greil R, *et al.* on behalf of the Austrian Breast and Colorectal Cancer Study Group. Predicting distant recurrence in receptor-positive breast cancer patients with limited clinicopathological risk: using the PAM50 Risk of Recurrence score in 1478 postmenopausal patients of the abcsg-8 trial treated with adjuvant endocrine therapy alone. *Ann Oncol* 2014;25:339–45.

37. Vieira AF, Schmitt F. An update on breast cancer multigene prognostic tests—emergent clinical biomarkers. *Front Med (Lausanne)* 2018;5:248.

38. Mischel PS, Cloughesy TF, Nelson SF. dna-microarray analysis of brain cancer: molecular classification for therapy. *Nat Rev Neurosci* 2004;5:782–92.

39. Terashima M, Maesawa C, Oyama K, *et al.* Gene expression profiles in human gastric cancer: expression of maspin correlates with lymph node metastasis. *Br J Cancer* 2005;92:1130–6.

40. Koh SS, Opel ML, Wei JP, *et al.* Molecular classification of melanomas and nevi using gene expression microarray signatures and formalin-fixed and paraffin-embedded tissue. *Mod Pathol* 2009;22:538–46.